Extended Embedded Depth Using Cascaded Resonators Near-field WPT System with High Efficiency for Biomedical Implants

Mohamed Aboualalaa[1,2], Ramesh K. Pokharel[1], Takana Kaho[3]
[1]Graduate School of Information Science and Electrical Engineering, Kyushu University, Japan
[2]Microstrip Department, Electronics Research Institute, Egypt
[3] Shonan Institute of Technology, Japan
m.aboualalaa@gmail.com, pokharel@ed.kyushu-u.ac.jp

***Abstract*—A novel multiple cascaded resonators wireless power transfer (WPT) design is proposed to provide an extended implanted depth for biomedical implants. Symmetrical four cascaded resonators are utilized in Tx/Rx to obtain high power transfer efficiency (PTE); each resonator consists of two concentric rectangular loops. KQ-product is calculated for a single resonator and compared with the four resonators WPT; four cascaded resonators achieve higher KQ-product value and produce a maximum measured PTE of 89.5% at a transfer distance of 20 mm. Then, the proposed WPT is tested with human tissue to provide a measured PTE of 76% and 63% at a transfer distance of 15 and 20mm, respectively. Specific absorption rate (SAR) is calculated to estimate the maximum operating power of the source and receiver that guarantees working within the safety standard levels of RF exposure.**

***Keywords*— Multiple cascaded resonators, power transfer efficiency (PTE), specific absorption rate (SAR), wireless power transfer (WPT).**

I. INTRODUCTION

Recently, wireless power transfer became a powerful technology due to its importance in wirelessly powering several devices such as mobile phones, portable electronic devices, electric vehicles, and many biomedical implants [1]-[3]. Several approaches have been investigated for maximizing the PTE between the transmitters and receivers of the conventional single input single output (SISO) WPT systems [4, 5] to obtain efficient WPT systems. A structure of two concentric open-loop spiral resonators (OLSRs) was proposed in [4] to improve the coupled magnetic field and transfer efficiency. A planar L-shape transmitter is introduced in [5] for an inductive coupled resonance where a second transmitting resonant coil is attached to form L-shape Tx for further power transfer improvement. In [6]-[8], intermediate resonators are exploited to improve the mutual coupling between the transmitters and receivers, which in turn increases the PTE between the Txs and Rxs. Nevertheless, the previous-mentioned SISO WPT systems do not give high enough power transfer efficiencies. Moreover, some works use three-dimensional structures for implementing the Txs and Rxs, which are unsuitable for many electronic devices. Furthermore, other works give high efficiency but at a relatively short transfer distance between the Tx and Rx.

In biomedical applications, the main issue that faces the WPT designers is how to obtain a high PTE at relatively large embedded transfer distances, which is required to transfer much power to deep biomedical implants with lower exposure time for RF waves [9]- [15]. [9]- [13] tried to get high PTE. However, the implanted distances for these designs are not large enough. [14] achieves a high embedded depth, but it provides a low measured PTE. [15] also achieves a high PTE with a high transfer distance. Nevertheless, it uses large sizes for Tx/Rx and provides low received power operation to ensure the system works under the standard limits for SAR, which limits its applications. The proposed WPT design uses multiple cascaded resonators to provide a high PTE as well as achieves large embedded depth. The drawback of the proposed WPT design is that Rx has a relatively large area. However, it is still smaller than [15]. Besides, there are some devices that require a relatively large Rx size, such as ventricular assist devices or pacemakers [16]. The main requirements of these devices are higher values of PTE and implanted depth, and our proposed design achieves both of them.

II. PROPOSED WPT CASCADED RESONATORS SYSTEM

The idea for the proposed WPT design comes from the analogy with the series-fed antenna array, where a series-fed antenna array is used to increase the antenna's radiation area, which improves the radiation performance. In the same way, we use series-fed cascaded resonators in the near-field to increase the coupled area between the Tx and Rx. We began with series-fed cascaded elements; then, we conformed it to form a closed loop, as shown in Fig. 1. We investigated a wide study of several resonators (stepped impedance, split ring, etc.). However, the proposed two concentric loops structure gave better KQ-product results. A study of KQ-product and maximum power transfer for one, two, three, and four resonators was investigated by calculating the KQ product as well as the maximum power transfer efficiency. When the Tx and Rx are symmetrical, maximum efficiency and KQ product for N-element cascaded system can be estimated as in (1) and (2) [17]. Where M is the mutual coupling between two symmetric elements, and R is the loss resistance.

$$PTE_{max} = 1 - \frac{2}{1+\sqrt{1+\chi^2}} \quad (1)$$

$$\chi = \sum_{n=1}^{N} \frac{\omega M_n}{R_n} \quad (2)$$

Fig. 2 shows the KQ product and maximum PTE of different numbers of resonators versus the frequency at different transfer distances. By decreasing the transfer distance (d), the system gives better results for the KQ product and maximum efficiency. However, d= 20mm is chosen with four

cascaded resonators system to give higher KQ-product and maximum power transfer efficiency. When d is lower than 20 mm, over-coupling occurs and the efficiency begins to decay at the operating frequency. Table 1 summarizes the KQ values at 70MHz and d= 20mm. It is clear from Table 1 that using WPT with four resonators gives higher KQ product and maximum power transfer efficiency than using one, two, or three resonators. When the number of resonators is one (N=1), the KQ product and maximum PTE are 10.6, and 82.8%, respectively. Whereas, after using four resonators (N=4), KQ product and maximum PTE reach 19.4, and 90.2%, respectively. Therefore, four cascaded resonators system is employed through our study at a transfer distance of 20mm.

Tx/Rx of the proposed cascaded resonators WPT system comprises four series-connected resonators. Each resonator consists of two concentric loops. The dimensions of each resonator are 5mm × 18mm. The geometrical parameters of the whole WPT system are L= 30mm, L_1= 18mm, W_1= 1.5mm, W_2= 0.4mm, W_3= 0.5mm, W_4= 1mm, W_5= 0.5mm, W_6= 1.5mm, W_7= 1mm, and W_8= 5mm. The Tx and Rx of the proposed WPT system are printed on a thin substrate, Rogers RT/Duroid RO3003 substrate with a substrate thickness (h) of 0.76 mm, dielectric constant (ε_r) of 3, copper thickness (t) of 0.0017 mm and a dielectric loss tangent (tanδ) of 0.0013. The fabricated prototype of the four cascaded resonators system is shown in Fig 1. Two capacitors (C_1= 20 pF and C_2= 85 pF) are utilized for achieving the matching. During the measurements, high-quality factor lumped capacitors (GJM series by Murata electronics) are utilized.

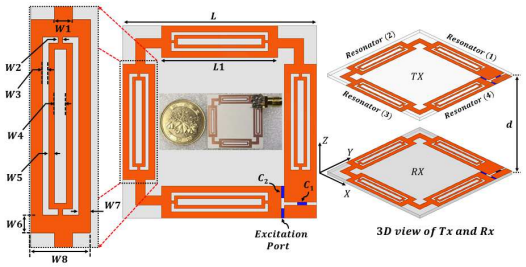

Fig. 1. Geometry of the proposed cascaded WPT system.

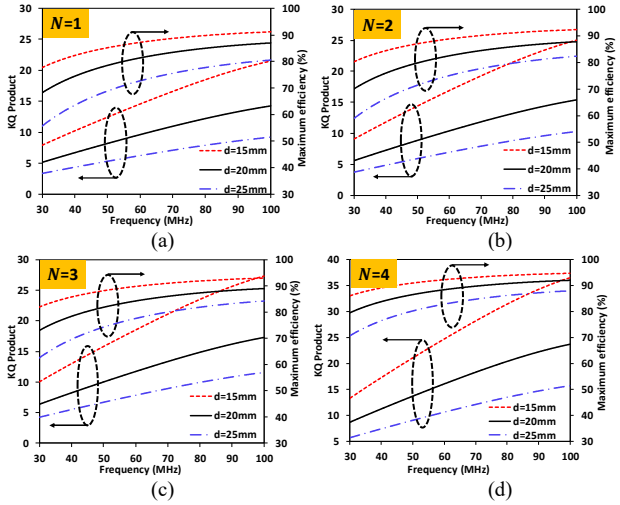

Fig. 2. KQ-product and maximum PTE for (a) single resonator (N=1), (b) two resonators (N=2), (c) three resonators (N=3), and (d) four resonators (N=4).

Table 1. KQ product and maximum efficiency at 70 MHz, and transfer distance of 20mm.

No. / Parameter	*N=1*	*N=2*	*N=3*	*N=4*
KQ-product	10.6	11.86	13.38	19.4
PTE_{max}	82.8	84.5	86.12	90.2

III. Experimental Results and Discussion

A. Experimental Results of Multiple resonators WPT System

The power transfer efficiency is calculated from the s-parameters as PTE=$|S_{21}|^2$. The proposed WPT system introduces simulated and measured efficiencies of 90.4% and 89.5% at 71 MHz and 70 MHz, respectively. Fig. 3(a) shows the simulated and measured efficiency versus the operating frequency. Moreover, a study for the efficiency versus the transfer distance (d) between the Tx and Rx is executed as illustrated in Fig. 3(b). The proposed WPT design gives a maximum efficiency at d=20mm. Then, with increasing the transfer distance, the efficiency decreases until it reaches about 5% at d=50mm.

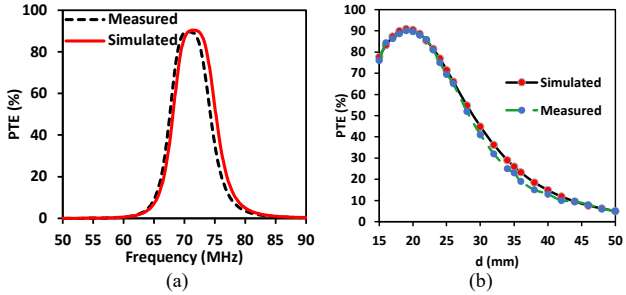

Fig. 3 Measured and simulated results of PTE (a) PTE versus the operating frequency, and (b) PTE versus the transfer distance between the Tx and Rx.

B. Implanted WPT

Since the proposed WPT was designed to be implanted inside the human body, it is necessary to imitate the natural working environment to ensure performance reliability. Consequently, a numerical three-layer phantom (skin, fat, and muscle) was employed with an overall dimension of 70×70×50 mm^3, as illustrated in Fig. 4 (a). Considering that the electrical properties of the human body are frequency dependent, the average values of these properties at the operating frequency are assigned to each layer with reference to [18] and listed in Table 2. The Rx is placed in the muscle layer, while the Tx is fixed on the top of the skin layer. Fig. 4(b) displays the numerical and measured results of the PTE versus the frequency; two implanted depths are investigated (d=15 and 20 mm). At d=15mm, the system provides a high measured PTE of 76%. By increasing the embedded depth, measured PTE starts to decay to 63% d=20mm. In addition, the measured PTE versus the embedded depth is investigated, as clear in Fig. 4(c); measured PTE ranges from 76% at d=15 mm to 40% at d=25mm.

Due to the high magnetic coupling of the proposed system, the coupled power can be delivered to the implanted Rx at higher transfer distances, compared with many proposed WPT systems [9-15], without much decay of the PTE. Through the

measurements, the Rx is implanted inside two slices of chicken meat, as shown in Fig. 4(d).

Table 2. Human body parameters at 70 MHZ.

Tissue	ε_r	Conductivity σ (S/m)	Loss Tan.
Skin	74.2	0.4948	1.7122
Fat	6.3986	0.0355	1.424
Muscle	70.752	0.69197	2.5115

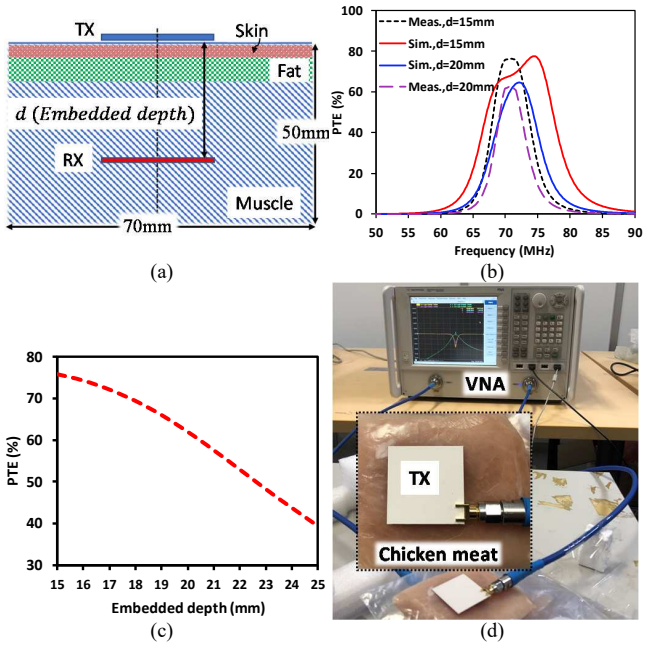

Fig. 4. Characteristics of the implanted Rx(a) structure (b) numerical and measured PTE, (c) PTE versus embedded depth, and (d) measurements setup.

C. SAR Calculations and Safety Considerations

The SAR is calculated to estimate the maximum safe power for the proposed WPT system when the Rx is implanted inside the human tissue for safety considerations. According to the IEEE Std. C95.1-2019 [19] for human safety standards, the 1-g average SAR level should be less than 1.6 W/kg. To fulfill the IEEE SAR regulations using the proposed WPT design, the transmitted power of the Tx should be less than 200 mW at 70 MHz. On the other side, the maximum delivered input power to the Rx should also be lower than 96 mW at the same operating frequency. Fig. 5(a) displays the changing of SAR levels when the transmitted power and received power changed from 50 mW to 250 mW. Fig. 5(b) shows the SAR distribution at 70 MHz. SAR values are determined from the SAR definition as in (1), where σ is the tissue conductivity (S/m), E is the induced electric field (V/m), and ρ is the tissue density (Kg/m^3). Electromagnetic (EM) simulations were performed using ANSYS High-Frequency Structure Simulator (HFSS).

$$SAR = \frac{\sigma |E|^2}{\rho} \quad (3)$$

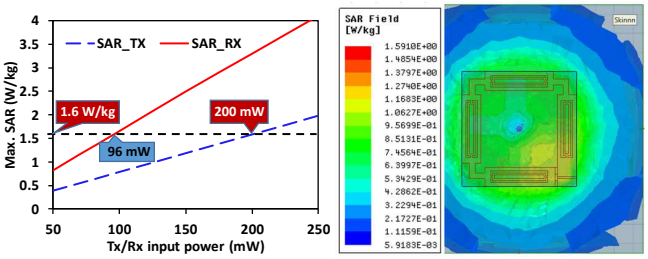

Fig. 5. (a) changing SAR levels with the transmitted and received input power, and (b) SAR distribution at 70MHz.

D. Misalignment Study

Practically, the Tx is fixed on the surface of the body, while the Rx is inside implanted inside the body. Thus, there is a probability of planar or angular misalignment between the Tx and Rx, as illustrated in Fig. 6. Consequently, the two cases of the misalignments are studied at the two values of the transfer distance (d=15 and 20 mm). Figs. 6(b), and (c) display the strong immunity for the proposed WPT system against angular misalignments, where angular misalignments have little effect on the PTE at the two investigated distances.

Table 3. Comparison between the proposed WPT and other recently published WPT designs.

Reference	Geometry	Tissue	f_0 (MHz)	ATX (mm^2)	ARX (mm2)	d(m m)	Measured PTE (%)	Maximum source power (mW)	Maximum receiving power (mW)
[9]	Planar split-ring loops	pork	403	39.6×39.6	25.5×25.5	6	57.9	159	92
[10]	UHF antenna	Saline	13.56	85×85	25×25	16	17	100	17
[11]	Planar ring resonator	pork	403	20.48×20. 48	15.48×15. 48	5	20.54	38	7.77
[12]	Metamaterial inspired geometry	chicken	50	20×20	10×10	10	64	168	-
[13]	Stacked MRR metamaterial	chicken	50	20×20	7×7	9	51	130	-
[14]	Square coils with Metamaterial	Skin gel	430	40×40	10×10	20	2.51	-	-
[15]	Wire coils	-	5	70×70	35×35	20	80	-	18
This work	Cascaded resonators	chicken	71	30×30	30×30	20/1 5	63/76	200	96

While the planar misalignment has more effect on the PTE due to the changing in the coupled magnetic field between the Tx and Rx, as shown in Fig. 6(a). However, the design still provides PTE over 50 % even if the Rx is shifted by 10 mm. Table 3 shows a comparison between the proposed WPT design and other recently published WPT systems.

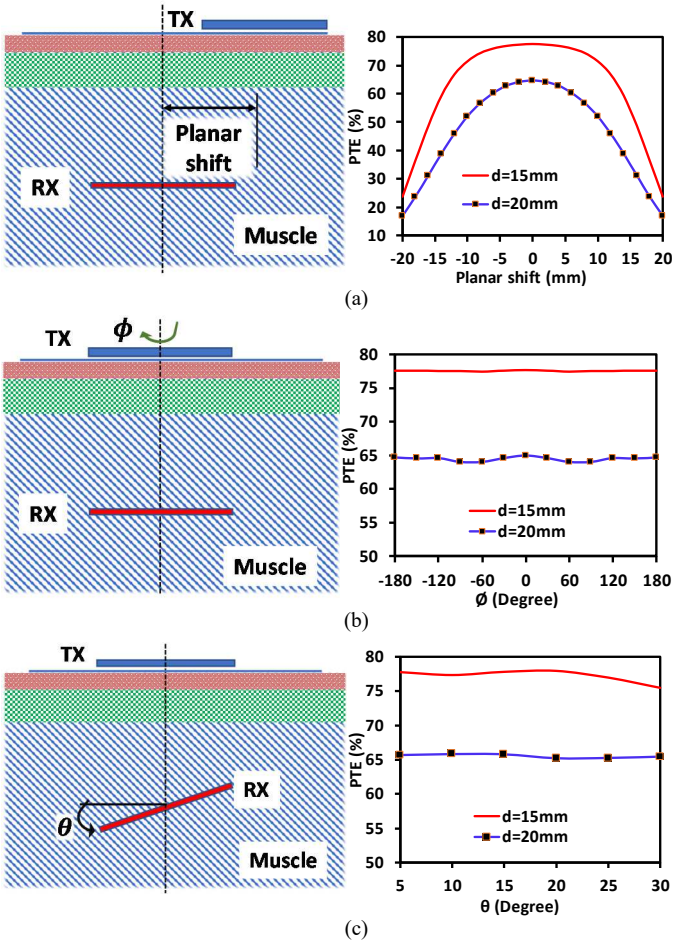

Fig. 6. Misalignment study for the proposed implanted WPT design (a) planar shift, (b) angular shift around the center axis for the Tx and Rx (∅), and (c) angular shift around Rx's center (θ).

IV. Conclusion

A cascaded four-resonator WPT design for implanted biomedical applications is introduced in this paper. Firstly, the KQ product study for single and multiple resonators was discussed to show the enhancement in the maximum PTE after using the multiple cascaded resonators. Then, this design is implanted in human tissue to show the power transfer performance after considering the tissue characteristics. The design gives high PTE at deeply implanted distances. Finally, a misalignment study is executed, and the obtained results reveal a good performance of the proposed implanted design when it undergoes the misalignment issues.

Acknowledgment

This work was supported in part by the Japan Society for the Promotion of Science [Post-Doctoral Fellowships for Research in Japan (Standard)] under Grant 21F51046, in part by the MIC/SCOPE Grant Number: JP215010003, in part by the Keysight Technologies Japan, Ltd., and in part by the VLSI Design and Education Center (VDEC) of the University of Tokyo.

References

[1] A. M. Dizqah, B. Lenzo, A. Sorniotti, P. Gruber, S. Fallah, and J. De Smet, "A Fast and parametric torque distribution strategy for four-wheel-drive energy-efficient electric vehicles," *IEEE Trans. Ind. Electron.*, vol. 63, no. 7, pp. 4367–4376, 2016.

[2] J. Wang et al., "A 403 MHz wireless power transfer system with tuned split-ring loops for implantable medical devices," *IEEE Trans. Antennas Propag.*, vol. 70, no. 2, pp. 1355–1366, 2022.

[3] M. Aboualalaa, H. Elsadek, and R. K. Pokharel, "WPT, recent techniques for improving system efficiency," in Wireless Power Transfer–Recent Development, Applications and New Perspectives, InTechOpen, 2021.

[4] M. Aboualalaa, I. Mansour, A. Barakat, K. Yoshitomi, and R. K. Pokharel, "Improvement of magnetic field for near-field WPT system using two concentric open-loop spiral resonators," *IEEE Microw. Wirel. Components Lett.*, no. 2, pp. 1–4, 2020.

[5] Z. Liu, Z. Chen, J. Li, Y. Guo, and B. Xu, "A planar L-shape transmitter for a wireless power transfer system," *IEEE Antennas Wirel. Propag. Lett.*, vol. 16, pp. 960–963, 2017.

[6] K. Lee and S. H. Chae, "Power transfer efficiency analysis of intermediate-resonator for wireless power transfer," *IEEE Trans. on Power Electronics*, vol. 33, no. 3, pp. 2484-2493, 2018.

[7] D. Brizi, J. P. Stang, A. Monorchio and G. Lazzi, "On the design of planar arrays of nonresonant coils for tunable wireless power transfer applications," *IEEE Trans. Microw. Theory Techn.*, vol. 68, no. 9, pp. 3814-3822, Sept. 2020.

[8] M. Aboualalaa, I. Mansour and R. K. Pokharel, "Experimental study of effectiveness of metasurface for efficiency and misalignment enhancement of near-field WPT system," *IEEE Antennas Wireless Propag. Lett.*, vol. 21, no. 10, pp. 2010-2014, Oct. 2022.

[9] J. Wang et al., "A 403 MHz wireless power transfer system with tuned split-ring loops for implantable medical devices," *IEEE Trans. Antennas Propag.*, vol. 70, no. 2, pp. 1355-1366, Feb. 2022.

[10] A. Sharma, E. Kampianakis and M. S. Reynolds, "A dual-band HF and UHF antenna system for implanted neural recording and stimulation devices," *IEEE Antennas Wireless Propag. Lett.*, vol. 16, pp. 493-496, 2017.

[11] G. Monti, M. V. De Paolis, L. Corchia, and L. Tarricone, "Wireless resonant energy link for pulse generators implanted in the chest," *IET Microw., Antennas Propag.*, vol. 11, no. 15, pp. 2201–2210, Oct. 2017.

[12] R. K. Pokharel, A. Barakat, S. Alshhawy, K. Yoshitomi, and C. Sarris, "Wireless power transfer system rigid to tissue characteristics using metamaterial inspired geometry for biomedical implant applications" Scientific Reports, 11(1), 1–10, 2021.

[13] S. Alshhawy, A. Barakat, R. K. Pokharel and K. Yoshitomi, "Low magnetic loss metamaterial based miniaturized WPT system for biomedical implants," IEEE MTT-S International Microwave Symposium - IMS, pp. 275-278, 2022.

[14] L. Li, H. Liu, H. Zhang, and W. Xue, "Efficient wireless power transfer system integrating with metasurface for biological applications," *IEEE Trans. Ind. Electron.*, vol. 65, no. 4, pp. 3230–3239, Apr. 2018.

[15] M. Machnoor, E. S. G. Rodríguez, P. Kosta, J. Stang, and G. Lazzi, "Analysis and design of a 3-coil wireless power transmission system for biomedical applications," *IEEE Trans. Antennas Propag.*, vol. 67, no. 8, pp. 5012–5024, Aug. 2019.

[16] Y. Pya et al., "First human use of a wireless coplanar energy transfer coupled with a continuous-flow left ventricular assist device," *J. Heart Lung Transplantation*, vol. 38, no. 4, pp. 339–343, Apr. 2019.

[17] Q. Duong, and M. Okada, "Maximum efficiency formulation for multiple-input multiple-output inductive power transfer systems". *IEEE Trans. Microw. Theory Techn.*, vol. 66, no 7, pp. 3463–3477, 2018.

[18] http://niremf.ifac.cnr.it/tissprop/htmlclie/htmlclie.php

[19] IEEE Standard for Safety Levels with Respect to Human Exposure to Electric, Magnetic, and Electromagnetic Fields, 0 Hz to 300 GHz, Standard IEEE C95.1-2019, Oct. 2019.